

ARTICLES

Ultraviolet Photochemistry of Diacetylene with Alkynes and Alkenes: Spectroscopic Characterization of the Products

Caleb A. Arrington,[†] Christopher Ramos, Allison D. Robinson, and Timothy S. Zwier*

Department of Chemistry, Purdue University, West Lafayette, Indiana 47907-1393

Received: October 5, 1998

The primary reaction products formed when metastable diacetylene ($C_4H_2^*$) reacts with ground-state diacetylene (C_4H_2), ethylene (C_2H_4), and propene ($CH_3-CH=CH_2$) have been spectroscopically characterized using a laser pump–probe scheme. Reaction is initiated in a constrained expansion which limits reaction times to about 20 μ s. The molecular structures of the C_6H_2 product formed in the $C_4H_2^* + C_4H_2$ reaction is identified from its R2PI spectrum and two-photon ionization threshold (9.49 ± 0.01 eV) as triacetylene ($H-C\equiv C-C\equiv C-H$). The analogous scans of the C_8H_2 product show a clear two-photon ionization onset at 9.09 ± 0.02 eV, but little resolved vibronic structure above this threshold, consistent with its assignment as tetraacetylene. The R2PI spectra of the C_6H_4 product formed in the reactions of $C_4H_2^*$ with C_2H_4 and $CH_3-CH=CH_2$ lead to an identification of this product as 1-hexene-3,5-diyne ($CH_2=CH-C\equiv C-C\equiv CH$). The C_7H_6 product formed in the reaction of $C_4H_2^*$ with $CH_3-CH=CH_2$ possesses an R2PI spectrum close to that of 1-hexene-3,5-diyne, supporting its identification as a methylated derivative with the same ene–diyne structure. Two C_7H_6 isomers meet this criterion, 5-heptene-1,3-diyne ($CH_3-CH=CH_2-C\equiv C-C\equiv C-H$) and 2-methyl-1-hexene-3,5-diyne ($H_2C=C(CH_3)-C\equiv C-C\equiv C-H$), between which we cannot distinguish. Implications for the mechanisms for these $C_4H_2^*$ reactions are discussed.

I. Introduction

Throughout much of the ultraviolet, excitation of diacetylene (C_4H_2 , $H-C\equiv C-C\equiv C-H$) is to bound levels below the lowest dissociation threshold of the molecule (~ 133 kcal/mol).¹ At the same time, intersystem crossing is efficient, producing metastable triplet states which are responsible for much of diacetylene's photochemistry.² Recent studies by our group^{3–7} have uncovered a rich chemistry for metastable diacetylene ($C_4H_2^*$) with a wide range of unsaturated hydrocarbons and nitriles. The efficient photochemical polymerization of C_4H_2 complicates the detection of the primary products of $C_4H_2^*$ reactions.² Our group has used a scheme whereby excitation of diacetylene occurs in a constrained expansion which limits the number of collisions following photoexcitation and thereby enables the detection of primary products of $C_4H_2^*$ reactions.

In earlier reports, we have studied the reactions of metastable diacetylene with ground-state diacetylene,^{3,4} acetylene (C_2H_2),⁵ ethylene (C_2H_4), propene ($CH_3-CH=CH_2$), propyne ($CH_3-C\equiv CH$),⁶ and 1,3-butadiene ($H_2C=CH-CH=CH_2$).⁷ In much of this work, vacuum ultraviolet (VUV) photoionization at 118 nm (10.5 eV) has been used as a gentle, general photoionization scheme. When coupled with time-of-flight mass spectroscopy, it has provided information on the relative product yields from the ion abundances so formed. In the end, however, the chemical structures of the products is inferred from the mass-to-charge ratio. As one proceeds toward more complex reaction mixtures,

the ambiguity in assigning a given mass ion to a given product structure grows and spectroscopic detection of the products becomes increasingly important.

We have recently extended our capabilities to include resonance-enhanced multiphoton ionization by which one can determine the ultraviolet spectra of those products with accessible excited electronic states. In the recent study of the reaction $C_4H_2^* + 1,3$ -butadiene,⁷ the C_6H_6 and C_8H_6 products were identified by such means as benzene and phenylacetylene. This surprising result constitutes a first example of metastable diacetylene's role in aromatic ring-forming reactions. The fact that it was unanticipated highlights the importance of spectroscopically characterizing the reaction products whenever possible in order to determine their structures unambiguously.

Furthermore, many of the reaction products formed are rather exotic species which cannot easily be made or handled by other means. Hence, the chemical reactions of diacetylene with hydrocarbons and nitriles offers an unusual opportunity to study the gas-phase spectroscopy of various poly-yne, enyne, cumulene, radical, and aromatic species.

In the present work, resonant two-photon ionization (R2PI) is used to determine the ionization thresholds and record R2PI spectra for several key enyne and poly-yne products of $C_4H_2^*$ reactions. In particular, the C_6H_2 and C_8H_2 products from the $C_4H_2^* + C_4H_2$ reaction are identified by such means as triacetylene ($H-(C\equiv C)_3-H$) and tetraacetylene ($H-(C\equiv C)_4-H$), respectively. The C_6H_4 product which dominates the product mass spectra in the reactions of $C_4H_2^*$ with ethylene and propene is assigned from its R2PI spectrum as 1-hexene-3,5-diyne. Finally, the C_7H_6 product from the $C_4H_2^* +$ propene

* Author to whom correspondence should be addressed.

[†] Present address: Department of Chemistry, Central Washington University, Ellensburg, WA 98926-7539.

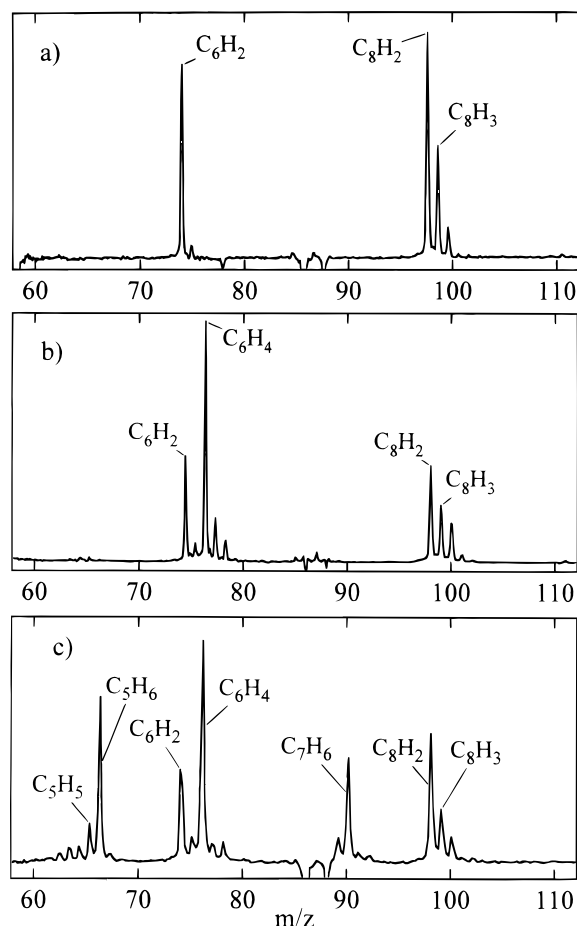


Figure 1. VUV photoionization difference mass spectra (photoexcitation laser on – photoexcitation laser off) highlighting the primary photoproducts of the reactions (a) $C_4H_2^* + C_4H_2$, (b) $C_4H_2^* + C_2H_4$, and (c) $C_4H_2^* + CH_3CH=CH_2$. Products were ionized with 118 nm radiation. The reactant mass peaks (not shown) are approximately 200 times larger than those displayed.

reaction possesses an R2PI spectrum closely similar to that of the C_6H_4 product, consistent with retention of the ene-diyne structure in this product.

II. Experimental Section

The experimental apparatus and methods have been described previously.^{4,7} In the present experiments, gas mixtures of 1–3% C_4H_2 and 3–10% ethylene or propene in helium were expanded through a short reaction tube (1 cm in length, 2 mm diameter) affixed to the orifice of a pulsed valve. As the reaction mixture makes the 20 μ s traversal of this tube, photochemistry is initiated using the doubled output (0.5 mJ/pulse) of an excimer (XeCl)-pumped dye laser which is tuned to the $2^1_06^1_0$ band of the $^1\Delta_u \leftarrow X^1\Sigma_g^+$ transition in diacetylene (231.5 nm, $\sigma_{abs}(2^1_06^1_0) = 3.2 \times 10^{-18}$ cm²/molecule).³ A few percent of the diacetylene molecules are excited by the laser. The excited singlet state is a doorway to the reactive triplet state through rapid intersystem crossing, either directly or mediated by the lower-energy $^1\Sigma_u^+$ state, producing high vibrational levels of the low-lying triplet states ($^3\Delta_u$ and/or $^3\Sigma_u^+$).^{2,4} Reaction then occurs from this metastable state(s) until molecular collisions cease outside of the reaction tube as the free expansion begins.

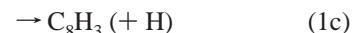
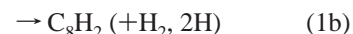
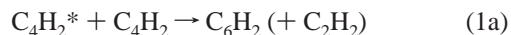
The gas mixture exiting from the photochemical source is photoionized in the extraction region of a time-of-flight mass spectrometer and mass-analyzed. In cases where general product detection is desired, photoionization is achieved using one-

photon vacuum ultraviolet photoionization at 118 nm (10.5 eV) produced by tripling the third harmonic of the Nd:YAG laser in xenon gas.^{4,8} The R2PI spectra and ionization threshold scans were recorded using the doubled output of a Nd:YAG-pumped dye laser (0.5 mJ/pulse). Scans over the wavelength range from 215 to 280 nm were achieved using the doubled output from four dyes (Coumarin 460, 480, 503, and 540A). Diacetylene was synthesized in our laboratory using procedures described earlier.^{4,5} It is stored and used as a dilute gas-phase mixture (1–5%) in helium.

III. Results and Analysis

Figures 1a–c present the VUV photoionization difference time-of-flight mass spectra of the $C_4H_2^*$ reactions with diacetylene, ethylene, and propene, respectively. The mass spectra of Figure 1 are the difference between a 1000-shot mass spectrum taken with the reactants exposed to the photochemical laser and a 1000-shot mass spectrum taken without the photochemistry laser present. The difference spectra highlight the photochemical products, and also largely compensate for the interference from the impurity 2-chloro-1-butene-3-yne ($m/z = 86,88$) present (in a 1:100 ratio with C_4H_2) from the synthesis of C_4H_2 . The mass signal due to this impurity produces a small negative subtraction which has been shown in earlier work⁵ to be photochemically inactive, suggesting a small difference in the transport of the gas mixture to the ionization region in the presence of the photoexcitation laser. Previous studies of the VUV photoionization of various poly-yne, enyne, and cumulene C_nH_m products have shown no evidence of fragmentation following photoionization at 118 nm.⁶ This photoionization wavelength (10.5 eV/photon) is above the ionization potential of most photoproducts, but below the first dissociation limit of the ion. Under these circumstances, the observed photochemical product ion masses reflect the nascent neutral species formed in the gas-phase reaction.

The major primary products from the $C_4H_2^*$ reactions with C_4H_2 , C_2H_4 , and C_3H_6 are labeled in the mass spectra of Figure 1a–c, respectively, with molecular formula determined from the mass-to-charge ratio, and confirmed by isotopic analysis of products formed from deuterated or partially deuterated reactants.^{4,6} In the $C_4H_2^* + C_4H_2$ reaction (Figure 1a, reaction 1), the dominant observed products are C_6H_2 and C_8H_2 , with C_8H_3 contributing as a minor product.



The products in parentheses are not directly observed (since they have ionization potentials above 10.5 eV), but are deduced from mass conservation coupled with thermodynamic constraints on further fragmentation. In our previous work, the C_6H_2 and C_8H_2 products were surmised to be triacetylene and tetraacetylene, respectively, using mass spectral data alone.^{3,4}

In the reactions of $C_4H_2^*$ with ethylene (Figure 1b) and propene (Figure 1c), diacetylene's self-reaction necessarily occurs in parallel with the reaction of interest. The relative intensities of the two sets of products can be controlled by adjusting the relative concentrations of C_4H_2 and alkene in the gas mixture. In neither reaction is there interference between the two sets of products, as confirmed by concentration studies. Clearly, C_6H_4 is the dominant product formed from the reactions

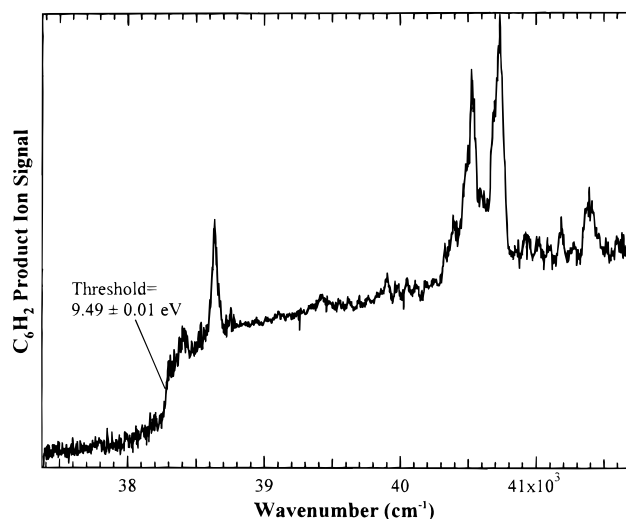


Figure 2. Resonant two-photon ionization scan of the C_6H_2 product from the $C_4H_2^* + C_4H_2$ reaction in the threshold region for two-photon ionization. The two-photon ionization threshold (9.49 ± 0.01 eV) is within experimental error of the known value for triacetylene (9.50 ± 0.02 eV).¹⁰ The sharp transitions appearing above threshold are part of the vibronic structure of the $S_2 \leftarrow S_0$ transition in C_6H_2 . See the text for further discussion.

of $C_4H_2^*$ with both C_2H_4 and $CH_3CH=CH_2$, motivating its spectroscopic characterization.

A. The C_6H_2 and C_8H_2 Products from the $C_4H_2^* + C_4H_2$ Reaction: The chemical reactions identified for $C_4H_2^* + C_nH_m$ typically produce large hydrocarbon products which result from what is formally the loss of a small, stable molecule from the reaction complex, whether H_2 , C_2H_2 , C_2H_4 , or CH_4 . In the $C_4H_2^* + C_4H_2$ reaction 1, H_2 loss (either as H_2 or $2H$) forms C_8H_2 while C_2H_2 loss produces C_6H_2 as the observable product. Based on thermodynamics, the most stable structures for the C_6H_2 and C_8H_2 products are triacetylene and tetraacetylene, respectively, but this has yet to be proved. From an energetic standpoint, for instance, a vinylidene-like C_6H_2 such as $H-C\equiv C-CH=C=C\equiv C$: could also be an accessible pathway for loss of C_2H_2 from the reaction complex.

The ultraviolet absorption spectrum of gas-phase triacetylene has been investigated at room temperature by Kloster-Jensen et al.⁹ The spectrum in the near-ultraviolet bears a close resemblance to that of C_4H_2 , but is shifted to longer wavelengths, as one might anticipate from a longer-chain poly-yne. The spectrum is dominated by long, intense Franck–Condon progressions in the $C\equiv C$ stretch at 2110 ± 10 cm^{-1} (2105 cm^{-1} in C_4H_2), built off two low-frequency bending modes. The ionization potential of triacetylene has been determined by photoelectron spectroscopy¹⁰ to be 9.50 ± 0.02 eV. In two-photon ionization, one anticipates an ionization threshold at half this energy, corresponding to 38310 ± 80 cm^{-1} (261.0 nm).

Figure 2 presents a multiphoton ionization scan through this wavenumber region while monitoring the $C_6H_2^+$ ion mass in the time-of-flight mass spectrum. The spectrum was recorded after photoexcitation of C_4H_2 through its $2^1_06^1_0$ transition at 231.5 nm, with pump–probe delay times set to photoionize the reaction products during their traversal of the extraction region of the time-of-flight mass spectrometer. A sharp threshold in ionization signal is observed at 38270 ± 40 cm^{-1} , corresponding to a two-photon ionization threshold of 9.49 ± 0.01 eV.¹¹ This is within experimental error of the accepted ionization potential for C_6H_2 .¹⁰

Furthermore, the sharp structure observed above the ionization threshold can be assigned to transitions in the ultraviolet

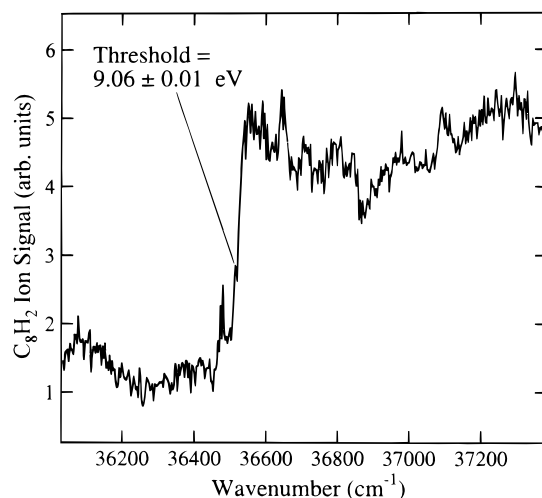


Figure 3. Resonant two-photon ionization scan of the C_8H_2 product from the $C_4H_2^* + C_4H_2$ reaction in the threshold region for two-photon ionization. The two-photon ionization threshold (9.06 ± 0.01 eV) is within experimental error of the known value for tetraacetylene (9.09 ± 0.02 eV).¹⁴

absorption spectrum of triacetylene by comparison with its known spectrum.^{9,12} The absorption spectrum of triacetylene, like diacetylene, is dominated by long progressions in ν_2 , the symmetric $C\equiv C$ stretch, with frequency 2110 cm^{-1} .^{9,12} In the room-temperature absorption spectrum, strong doublets⁹ appear at $38370/38580$ cm^{-1} and again at $40500/40700$ cm^{-1} . These doublets were assigned tentatively by Haink and Jungen¹² as $2^2_08^1_0/2^2_08^2_0$ and $2^3_08^1_0/2^3_08^2_0$, respectively, where ν_8 is a low-frequency $C\equiv C-H$ bending mode. In our one-color R2PI spectrum, the strong doublet at 40523 and 40733 cm^{-1} is the $2^3_08^1_0/2^3_08^2_0$ doublet. Similarly, the R2PI spectrum shows the $2^2_08^2_0$ transition at 38632 cm^{-1} (Figure 2), but the corresponding $2^2_08^1_0$ band is barely visible at 38420 cm^{-1} due to the small ionization cross section so near to the ionization threshold. The observed R2PI transitions have widths (full-width at half-maximum, fwhm) of 50 – 75 cm^{-1} , similar to the width observed for the corresponding $2^2_06^1_0$ band in C_4H_2 (39 cm^{-1}).¹³ Like diacetylene, this width is due to fast nonradiative processes in the excited state.

The fact that the triacetylene photochemical products show such a sharp ionization threshold reflects the significant cooling of photochemical products by the mild expansion accompanying the exit of the reaction mixture from the reaction tube. In the $C_4H_2^* +$ butadiene reaction,⁷ the benzene product formed showed negligible hot band intensity and a rotational temperature somewhere between 50 and 100 K.

The other stable product of the $C_4H_2^* + C_4H_2$ reaction is C_8H_2 , anticipated to be tetraacetylene. Tetraacetylene has a known ionization threshold of 9.09 ± 0.02 eV,¹⁴ corresponding to a two-photon ionization threshold at 36650 ± 80 cm^{-1} . Figure 3 presents a scan through this threshold region while monitoring the $C_8H_2^+$ mass channel under similar conditions used for the triacetylene scan of Figure 2. A clear threshold is observed for the $C_8H_2^+$ ion signal at 36530 ± 40 cm^{-1} , corresponding to a two-photon energy of 9.06 ± 0.01 eV, within experimental error of the accepted ionization potential for C_8H_2 . By comparison with triacetylene, the threshold spectrum of C_8H_2 is notable in two respects. First, the ion signal in two-photon ionization was significantly weaker than that for C_6H_2 , despite similar size signals under VUV photoionization. Second, scans which tune above threshold do not find any significant vibronic structure, unlike that for C_6H_2 . Both these features are a simple conse-

quence of the further red-shift of the UV absorption spectrum of C_8H_2 which places the two-photon ionization threshold above the strong Franck–Condon region of the one-photon $S_2 \leftarrow S_0$ transition where sharp transitions occur. Resonant enhancement is thereby weakened, and the sharp vibronic structure in the R2PI spectrum is no longer present.

B. The C_6H_4 and C_7H_6 Products Formed in the $C_4H_2^* +$ ethylene and propene Reactions. The dominant product formed in the reaction of metastable diacetylene with the ethylene and propene has a molecular formula of C_6H_4 . In earlier work, the C_6H_4 product from ethylene's reaction was proposed to be 1-hexene-3,5-diyne (**1**). This structure is consistent with the results of deuterium labeling studies, but does not rule out other C_6H_4 isomers, among which are *o*-, *m*-, and *p*-benzyne (**2–4**), *cis*- and *trans*-3-hexene-1,5-diyne (**5, 6**), and 3-methylene-1,4-diyne (**7**), shown below. Several of these isomers have known ionization potentials (**2** = 9.03 ± 0.05 eV,¹⁵ **5** = 9.10 ± 0.02 eV,¹⁰ **6** = 9.07 ± 0.02 eV), and the IP's of all isomers are anticipated to be well below the 10.5 eV photoionization cut-off for 118 nm radiation. The ultraviolet absorption spectra for **1, 2, 5**, and **7** have all been recorded in the gas phase.^{16,17} Of these, only **1** has well-resolved vibronic structure, with intense transitions at 270, 255, 242, and 230 nm.¹⁷

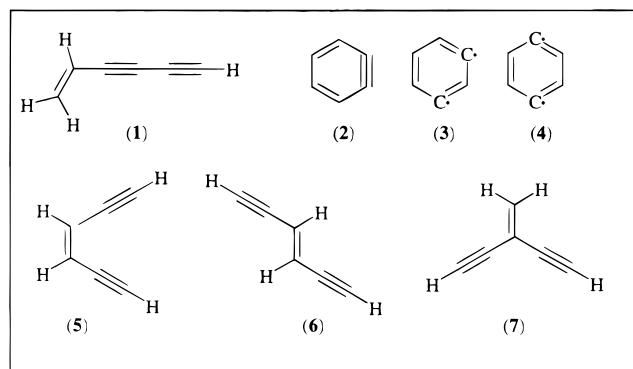


Figure 4 shows the corresponding ultraviolet R2PI spectrum of the C_6H_4 product from the $C_4H_2^* + C_2H_4$ reaction. Both the positions and intensities of the bands in the ultraviolet spectrum show a close correspondence with the spectrum of **1**, confirming that the C_6H_4 product from $C_4H_2^* + C_2H_4$ is indeed 1-hexene-3,5-diyne.¹⁷ The long progression in a 2080 cm^{-1} mode that dominates the spectrum can be assigned to the $C\equiv C$ stretch. Both the frequency of the vibration and Franck–Condon profile for this progression are very similar to that in the corresponding excited state of diacetylene (2105 cm^{-1}) and triacetylene (2110 cm^{-1}). In those cases, the $\pi-\pi^*$ excitation is predicted¹⁸ to produce a cumulene-like diradical excited-state structure ($HC=C=C=CH$ or $HC=C=C=C=CH$) whose longer $C-C$ bonds produce the long progression in the $C\equiv C$ stretch. One anticipates, on the basis of an analogy with diacetylene and triacetylene, that a similar $C\equiv C$ bond lengthening occurs upon $\pi-\pi^*$ excitation in 1-hexene-3,5-diyne, giving rise to the observed Franck–Condon progression.

One anticipates, on the basis of the close similarity of ethylene and propene, that the C_6H_4 product formed in the reaction of $C_4H_2^*$ with propene will also form 1-hexene-3,5-diyne. Indeed, as shown in Figure 5a, R2PI scans of the C_6H_4 product from this reaction show an spectrum identical to that in Figure 4a), consistent with formation of the 1-hexene-3,5-diyne isomer in this reaction as well.

Finally, we have successfully recorded an R2PI spectrum of the C_7H_6 product formed in the reaction with propene, shown

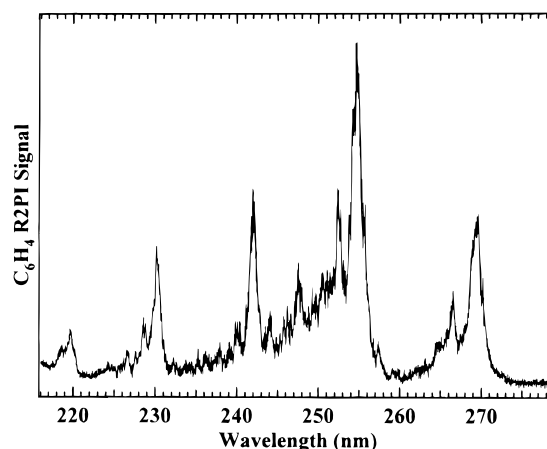


Figure 4. Resonant two-photon ionization scan of the C_6H_4 product from the $C_4H_2^* + C_2H_4$ reaction. The close correspondence with the UV absorption spectrum of 1-hexene-3,5-diyne (ref 17) confirms this as the isomeric structure formed in the $C_4H_2^* + C_2H_4$ reaction.

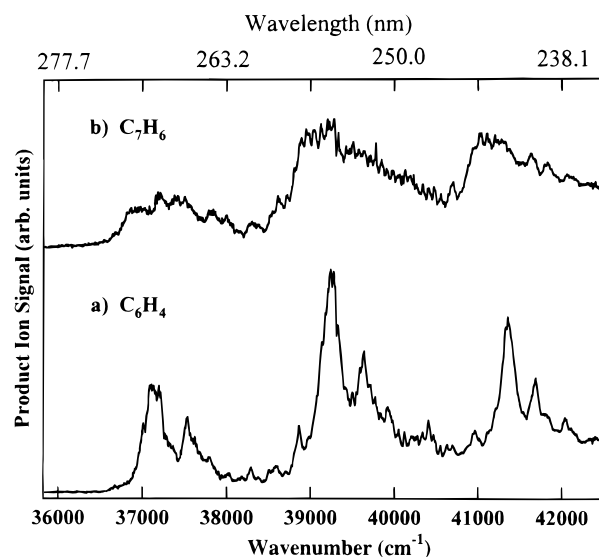


Figure 5. Resonant two-photon ionization scans of (a) the C_6H_4 and (b) the C_7H_6 products from the $C_4H_2^* +$ propene reaction. The C_6H_4 spectrum is identical to that in Figure 4, assigning the C_6H_4 product as 1-hexene-3,5-diyne. The C_7H_6 spectrum, by virtue of its close resemblance with the C_6H_4 product above it, shares the ene-diyne structure of the C_6H_4 product. Two methyl derivatives are consistent with the data. See the text for further discussion.

in Figure 5b). The spectrum bears a close resemblance to its C_6H_4 counterpart (Figure 5a). In particular, it too possesses a long Franck–Condon progression in the $C\equiv C$ stretch, with positions and spacing nearly identical to those in the C_6H_4 spectrum. Given this close correspondence, it seems very likely that the C_7H_6 isomer retains the same ene-yne-yne structure deduced for C_6H_4 (**1**). The implications in terms of mechanistic details are taken up in the discussion section.

IV. Discussion

The ionization threshold and R2PI vibronic structure of the C_6H_2 and C_8H_2 products formed in the $C_4H_2^* + C_4H_2$ reaction have been used to unambiguously identify these products as triacetylene ($H-C\equiv C-C\equiv C-C\equiv C-H$) and tetraacetylene ($H-C\equiv C-C\equiv C-C\equiv C-C\equiv C-H$), respectively. Such an identification provides confirming evidence for the reaction mechanism proposed earlier^{3,4} for their formation, reproduced in Figure 6a,b. Energetic constraints require that the C_2H_2 product

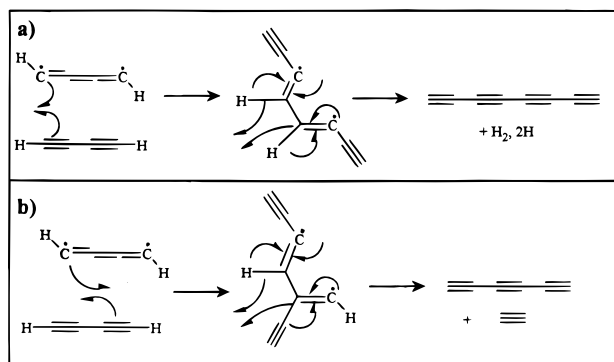
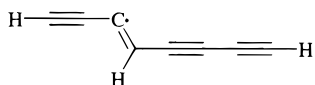


Figure 6. Proposed reaction mechanism for the formation of (a) tetraacetylene and (b) triacetylene in the $C_4H_2^* + C_4H_2$ reaction.

which accompanies triacetylene formation be formed intact (presumably as acetylene) and not as $C_2H + H$. For tetraacetylene, there is sufficient energy to form two hydrogen atoms rather than H_2 , depending on the extent of cooling of the $C_4H_2^*$ prior to reaction. In fact, our earlier work^{3,4} showed that when N_2 was used as buffer gas, C_8H_3 was formed in greater yield at the expense of C_8H_2 formation, consistent with reaction occurring from a lower-energy $C_4H_2^*$ distribution in the presence of N_2 .

Searches for R2PI absorptions of C_8H_3 over the 220–280 nm region were unsuccessful, leaving open the question of the precise structure of this free radical. However, given the strong evidence for tetraacetylene formation, it seems quite likely that the C_8H_3 product is formed in the same reaction pathway, with the adduct stabilized to energies where loss of a second H atom is not possible. This would form the following structure:



The R2PI spectrum of the C_6H_4 product formed from the $C_4H_2^* + \text{ethylene}$ reaction has provided an unambiguous assignment of this product as 1-hexene-3,5-diyne. This identification provides confirming evidence for the reaction mechanism shown in Figure 7a which was proposed previously on the basis of isotopic labeling results.⁶ The reaction is initiated by attack across the ethylenic double bond by the terminal carbon on the cumulene diradical. Loss of the interior hydrogens (either as an intact molecule or as two H atoms) from the reaction complex then leads to the observed product.

In the $C_4H_2^* + \text{propene}$ reaction, the route to C_6H_4 products has CH_4 or $CH_3 + H$ as coproducts. In our earlier study,⁶ we did observe the CH_3 product in VUV photoionization, confirming that dissociation by loss of CH_3 and H from the reaction complex does occur. Figure 7b presents a mechanism which forms 1-hexene-3,5-diyne by loss of CH_4 or $CH_3 + H$, proceeding by attack of the cumulene diradical on the interior carbon of propene.

What is less clear is the analogous pathway for C_7H_6 formation. As Figure 7b shows, the same intermediate which produces C_6H_4 could also form the 2-methyl-1-hexene-3,5-diyne C_7H_6 isomer (**8**) if H_2 (or $2H$) is lost rather than CH_4 (or $CH_3 + H$). Alternatively, attack on the exterior carbon of propene would produce the C_7H_6 isomer 1,3-diyne-5-heptene (**9**), as shown in Figure 7c. Since both isomers share the ene-diyne conjugated backbone with (**1**), differing only in the position of methyl substitution, one cannot easily distinguish between them on the basis of the R2PI spectrum. One might anticipate that (**9**) would be energetically preferred over (**8**) since the reaction

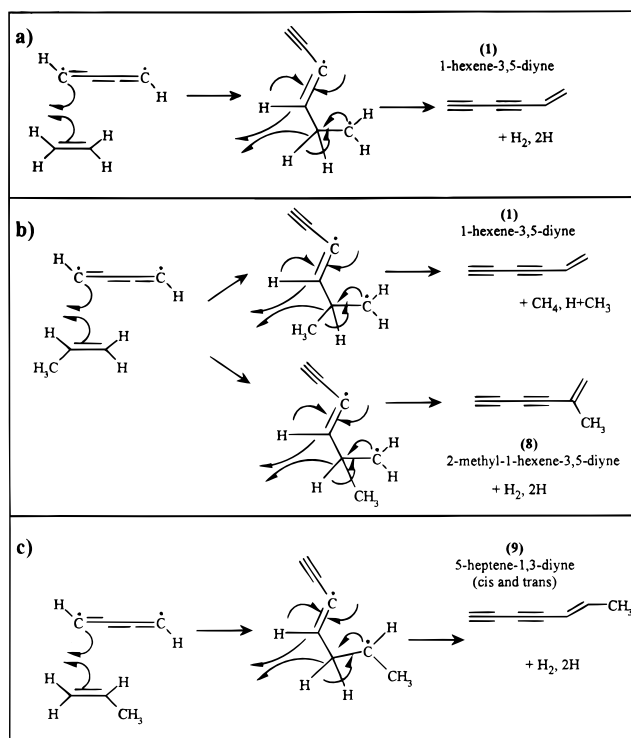


Figure 7. Proposed reaction mechanism for formation of (a) 1-hexene-3,5-diyne in the $C_4H_2^* + C_2H_4$ reaction, (b) 1-hexene-3,5-diyne (C_6H_4 , **1**) and 2-methyl-1-hexene-3,5-diyne (C_7H_6 , **8**) from the $C_4H_2^* + \text{propene}$ reaction, and (c) 1,3-diyne-5-heptene (C_7H_6 , **9**) from the $C_4H_2^* + \text{propene}$ reaction. The experimental data cannot distinguish between the two C_7H_6 isomers. See the text for further discussion.

complex which leads to (**9**) contains two secondary radical centers rather than a secondary and a primary radical, as in (**8**). Nevertheless, it is possible that both isomers contribute to the R2PI spectrum of Figure 5b, which could account for the denser vibronic structure appearing in the spectrum of Figure 5b by comparison to Figure 5a. Alternatively, the increased spectral congestion could arise in the spectrum of a single ene-diyne structure either from additional activity in low-frequency modes or increased state mixing accompanying attachment of a methyl group. In deciding between these possibilities, infrared spectra of the products would provide the necessary distinction, leaving room for further work.

V. Conclusion

Resonant two-photon ionization has been used to firmly establish the molecular structure of the C_6H_2 and C_8H_2 products from the $C_4H_2^* + C_4H_2$ reaction as triacetylene and tetraacetylene, respectively, and the C_6H_4 product from the $C_4H_2^* + \text{ethylene}$ and propene reactions as 1-hexene-3,5-diyne. The analogous R2PI spectrum of the C_7H_6 product formed in the $C_4H_2^* + \text{propene}$ reaction shows by its similarity with the spectrum of 1-hexene-3,5-diyne that it shares with it the same ene-diyne conjugated backbone. However, two isomers which differ in the position of methyl substitution are consistent with this constraint (**8** and **9**), and points out the limitation of ultraviolet spectroscopy in distinguishing isomeric structures in certain cases.

Acknowledgment. The authors gratefully acknowledge the Department of Energy, Office of Basic Energy Sciences, Division of Chemical Sciences for their support of this research under Grant No. DE-FG02-96ER14656.

References and Notes

- (1) Kiefer, J. H.; Sidhu, S. S.; Kern, R. D.; Xie, K.; Chen, H.; Harding, L. B. *Combust. Sci. Technol.* **1992**, 82, 101–130.
- (2) Glicker, S.; Okabe, H. *J. Phys. Chem.* **1987**, 91, 437.
- (3) Bandy, R. E.; Lakshminarayan, C.; Frost, R. K.; Zwier, T. S. *Science* **1992**, 258, 1630–1633.
- (4) Bandy, R. E.; Lakshminarayan, C.; Frost, R. K.; Zwier, T. S. *J. Chem. Phys.* **1993**, 98, 5362–5374.
- (5) Frost, R. K.; Zavarin, G.; Zwier, T. S. *J. Phys. Chem.* **1995**, 99, 9408–9415.
- (6) Frost, R. K.; Arrington, C. A.; Ramos, C.; Zwier, T. S. *J. Am. Chem. Soc.* **1996**, 118, 4451–4461.
- (7) Arrington, C. A.; Ramos, C.; Robinson, A. D.; Zwier, T. S. *J. Phys. Chem. A* **1998**, 102, 3315–3322.
- (8) Mahon, R.; McIlrath, T. J.; Myerscough, V. P.; Koopman, D. W. *IEEE J. Quantum Electron.* **1979**, QE-15, 444.
- (9) Kloster-Jensen, E.; Haink, H.-J.; Christen, H. *Helv. Chim. Acta* **1974**, 57, 1731–1744.
- (10) Bieri, G.; Burger, F.; Heilbronner, E.; Maier, J. P. *Helv. Chim. Acta* **1977**, 60, 2213.
- (11) Duncan, M. A.; Dietz, T. G.; Smalley, R. E. *J. Chem. Phys.* **1981**, 75, 2118–2125.
- (12) Haink, H.-J.; Jungen, M. *Chem. Phys. Lett.* **1979**, 61, 319–322.
- (13) Bandy, R. E.; Lakshminarayan, C.; Zwier, T. S. *J. Phys. Chem.* **1992**, 96, 5337–5343.
- (14) Allan, M.; Heilbronner, E.; Kloster-Jensen, E.; Maier, J. P. *Chem. Phys. Lett.* **1976**, 41, 228.
- (15) Zhang, X.; Chen, P. *J. Am. Chem. Soc.* **1992**, 114, 3147.
- (16) Schafer, M. E.; Berry, R. S. *J. Am. Chem. Soc.* **1965**, 87, 4497–4501.
- (17) Bohm-Gossl, T.; Hunsmann, W.; Rohrschneider, L.; Schneider, W. M.; Ziegenbein, W. *Chem. Ber.* **1963**, 96, 2504–2513.
- (18) Karpfen, A.; Lischka, H. *Chem. Phys.* **1986**, 102, 91.